# An *A Priori* Hot-Tearing Indicator Applied to Die-Cast Magnesium-Rare Earth Alloys

MARK A. EASTON, MARK A. GIBSON, SUMING ZHU, and TREVOR B. ABBOTT

Hot-tearing susceptibility is an important consideration for alloy design. Based on a review of previous research, an *a priori* indicator for the prediction of an alloy's hot-tearing susceptibility is proposed in this article and is applied to a range of magnesium-rare earth (RE)-based alloys. The indicator involves taking the integral over the solid fraction/temperature curve between the temperature when feeding becomes restricted (coherency) and that when a three-dimension network of solid is formed (coalescence). The hot-tearing propensity of Mg-RE alloys is found to vary greatly depending on which RE is primarily used, due to the difference in the solidification range. Mg-Nd alloys are the most susceptible to hot tearing, followed by Mg-Ce-based alloys, while Mg-La alloys show almost no hot tearing. The proposed indicator can be well applied to hot-tearing propensity of the Mg-RE alloys. It is expected that the indicator could be used as an estimation of the relative hot-tearing propensity in other alloy systems as well.

DOI: 10.1007/s11661-014-2272-7


## I. INTRODUCTION

HOT tearing is one of the most detrimental defects in castings, as the cracks compromise a cast component's structural integrity, can lead to a loss of pressure tightness, and can act as stress raisers aiding in the propagation of fatigue cracks or catastrophic failure. While hot tearing can be reduced by optimizing the design of the cast part in order to reduce areas of high stress intensity and to allow for more effective feeding of solidification shrinkage,[1] some alloys are intrinsically prone to hot tearing. Therefore, it is of critical importance to alloy design if the hot-tearing susceptibility of a potential alloy can be predicted.

The phenomenon of hot tearing is very complex as it is influenced by intrinsic alloy properties and process parameters. These factors include the solidification path,[2–5] wettability or interfacial energy of the solid phase by the liquid phase,[6] orientation of neighboring solid grains,[7] the viscosity of the liquid phase,[8] plastic deformation of the solid phase,[9–11] grain morphology features such as grain size and the dendrite arm spacing,[4,5,12–15] and cooling rates and casting speed or regime.[9,16,17] This means that comprehensive hot-tearing models are by nature very complex, as they need to involve a thermal solidification model, which then generate a stress/strain/strain rate response in a casting during solidification.[1,17–21] In turn, this needs to be coupled to a feeding model where the remaining liquid in a casting is required to feed through the mushy zone to accommodate the solidification shrinkage. Then, an essential criterion for tear initiation must be considered[22,23] and the point at which grain coalescence occurs identified.[24–26] While substantial progress has been made to develop comprehensive models, it is realized that for the purposes of alloy design, these models are more complex than is often necessary. Evidence of this is that even now, researchers are still using the much simpler hot-tearing models, such as the Clyne–Davies model of hot tearing to explain many results,[27–31] despite it being clear that it is unable to explain the hot-tearing response in many situations.[32–34]

Magnesium-rare earth (RE) alloys are of significant interest for their excellent properties, particularly for high-temperature creep-resistant and high-strength applications,[35–37] and as bio-absorbable alloys.[38] The most common RE elements are La, Ce, and Nd, and hence, these are being considered as the primary alloying elements, usually as misch metal. One of the most important considerations in the development of such alloys needs to be an understanding of the processability or castability of these alloys. It is well known that the hot-tearing susceptibility varies with alloy content through a lambda-curve relationship in most alloy systems.[4,29,30,39–41] At low alloy concentrations, the hot-tearing propensity is small; as the alloy content increases, it peaks, often within the range from 1 to 2 wt pct, and then reduces again at higher concentrations. Such data are currently not available for most Mg-RE systems although the Mg-Y[28] and Mg-Gd[42] systems have recently been evaluated.

MARK A. EASTON, formally Professor with the Department of Materials Engineering, CAST Co-Operative Research Centre, Monash University, Building 69, Clayton, VIC 3800, Australia, is now Deputy Head of School (Manufacturing and Materials), with the School of Aeorospace, Mechanical and Manufacturing Engineering, PO Box 71 Bundoora, VIC 3083, Australia. Contact e-mail: mark.easton@rmit.edu.au MARK A. GIBSON, Senior Principal Research Scientist, is with the CSIRO Process Science and Engineering, Clayton, VIC 3169, Australia. SUMING ZHU, Research Fellow, is with the Department of Materials Engineering, CAST Co-Operative Research Centre, Monash University. TREVOR B. ABBOTT, Director R&D, is with the Magontec Ltd., Level 8 139 Macquarie Street, Sydney, NSW 2000, Australia.

Manuscript submitted June 10, 2013.
Article published online April 1, 2014

**Table I. Important Features Obtained from the Mg-RE Binary Phase Diagrams[47]**

| RE | Atomic No. | Maximum Solid Solubility, $c_{ss}$ (Wt Pct RE) | Eutectic Composition, $c_{eut}$ (Wt Pct RE) | Eutectic Temperature [K (°C)] |
|---|---|---|---|---|
| La | 57 | 0.23 | 16.5 | 885 (612) |
| Ce | 58 | 0.74 | 20.5 | 863 (590) |
| Nd | 60 | 3.6 | 33 | 825 (552) |

Table from Ref. [43].

While RE elements have been traditionally grouped together under the one category, it is clear that each RE has quite different characteristics[43–47] related to their atomic number (Table I; Figure 1). Of the more common RE elements, which are investigated as alloying elements with Mg in this article, the Mg-La alloy system has the lowest solid solubility and eutectic composition and the highest eutectic temperature, while the Mg-Nd system has the highest solid solubility and eutectic composition and the lowest eutectic temperature—with the Mg-Ce system being in-between. These characteristics lead to: (1) differences in the precipitation response during creep, and hence creep properties;[44] (2) variations in the eutectic morphology and intermetallic identity, and hence mechanical and impact properties;[43,48] and (3) variations in the micro-galvanic behavior of the alloys, and consequently corrosion properties.[46]

This article has two foci: first, it is obtaining data on the hot-tearing behavior of the common RE elements, *i.e.*, La, Ce, and Nd in high pressure die-cast Mg alloys, and second, it is the development of a hot-tearing criteria *a priori* indicator that overcomes some of the issues related to the Clyne–Davies model, while maintaining its simplicity. The hot-tearing data of Mg-RE alloys are used to verify the applicability of the proposed indicator.

## II. EXPERIMENTAL METHODS AND RESULTS

### A. *Alloys*

A series of binary Mg-La, Mg-Ce, and Mg-Nd alloys were cast from commercially pure Mg and RE elements La, Ce, and Nd using a 250-tonne Toshiba cold chamber HPDC machine. The compositions of the alloys were nominally meant to range up to 6 wt pct, but the range obtained from measurements using inductively coupled plasma atomic emission spectroscopy (ICP-AES) shown in Table II (all compositions are given in wt pct unless otherwise stated) was less than this. Hence, an extra series of Mg-Nd alloys were prepared to extend the analysis to higher Nd levels, which given the hot-tearing results, was very important. In each casting, two cylindrical and one flat tensile sample were produced. The samples are the same as those for which the microstructures, and mechanical and creep properties were evaluated previously,[43,44] with the addition of a second series of high Nd content alloys.

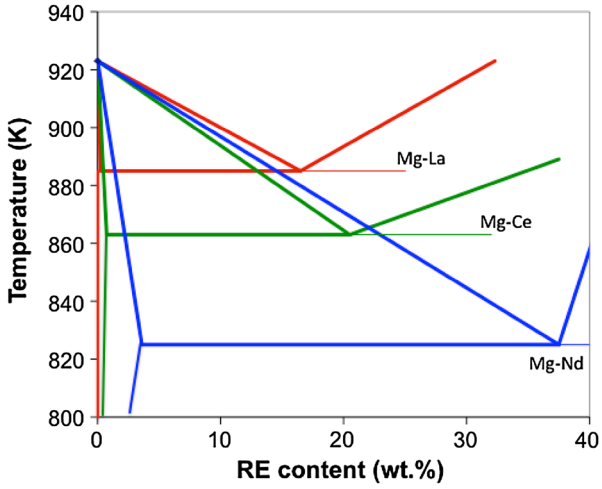


Fig. 1—Binary phase diagrams of Mg-La, Mg-Ce, and Mg-Nd overlayed assuming straight liquidus and solvus lines. The phase diagram data were obtained from Rokhlin.[47]

**Table II. RE Contents as Determined by ICP-AES in the Binary Mg-RE Alloys Used in this Work**

| La (Wt Pct) | Ce (Wt Pct) | Nd (Wt Pct) (Series 1) | Nd (Wt Pct) (Series 2) |
|---|---|---|---|
| 0.51 | 0.53 | 0.47 | 0.84 |
| 0.94 | 0.93 | 0.76 | 1.18 |
| 1.71 | 1.48 | 1.25 | 1.5 |
| 3.44 | 2.87 | 2.60 | 6.75 |
| 5.07 | 4.76 | 3.53 | 8.05 |

### B. *Hot-Tearing/Cracking Evaluation of HPDC Specimens*

Hot tearing is often measured using restrained bars of some sort, including "dog-bone" sections.[49,50] Tensile specimens provide an *in situ* test for evaluating hot tearing, which has been used previously.[51–53] However, in this study a more discerning scale was required to assess hot-tearing differences. A visual inspection of the surface of the flat samples was used to provide a hot-tearing criterion. While fine cracks were not able to be observed by the naked eye and therefore cannot be observed by this test, it was able to select out those alloys that have a high susceptibility to hot tearing and consequently decrease the amount of detailed metallography required. Since samples ranging from 25 to 30 were available for analysis, a statistically useful set of data could be obtained. A five-scale rating (0 to 4) was developed to evaluate the hot tearing in each sample as shown in Figure 2.

The rating scale was as follows:

(0) No cracks/dimples in the sample observed by the naked eye.
(1) Small observable dimple/s that require close examination to see.
(2) Dimple/s easily seen by the naked eye.
(3) Crack/s observed on the surface of the sample, but the sample was not broken.
(4) Sample broken.

Typical examples of rectangular tensile test specimens that display these characteristics on the outside as-cast surface are shown in Figure 3. It can be seen that occasionally very minor tears can be observed even in those samples given a rating of 0, although this is rare.

The hot-tearing index (HTI) was calculated as the mean value of the ratings given for each individual sample and a standard error, *i.e.*, the standard deviation divided by the square root of the number of samples measured, was also calculated as a measure of uncertainty.

## III. RESULTS

While all three series of alloys showed a peak in hot tearing, the concentration at which that peak occurred and the height of that peak varied (Figure 4). The Mg-Nd alloys showed the most severe hot-tearing behavior with a rating of approximately 1.0 and did not show an appreciable reduction in hot-tearing susceptibility until above 7 wt pct. Individual samples occasionally showed severe hot tearing with ratings of 3 or 4. Other results that have a large plateau for the maximum hot tearing, usually at the maximum value possible have been interpreted as being a truncated lambda-curve where the maximum cannot be measured.[54,55] In this case, the rating goes up to 4, and so it appears that it is not a truncated lambda-curve but a plateau.

The Mg-Ce alloys showed a substantially lower, but still significant, hot-tearing behavior with a peak at an HTI of approximately 0.5 at 0.5 to 1 wt pct. The Mg-La alloys showed almost no susceptibility to hot tearing with a peak of approximately 0.1 at approximately 1 to 2 wt pct La.


Fig. 2—Picture of a series of flat tensile test pieces each of which is representative of one of the categories in the hot-tearing scale defined (the reference number corresponding to the scale is indicated at the bottom of each). The white arrows indicate the surface dimples that are associated with internal cracking (see also Fig. 3).

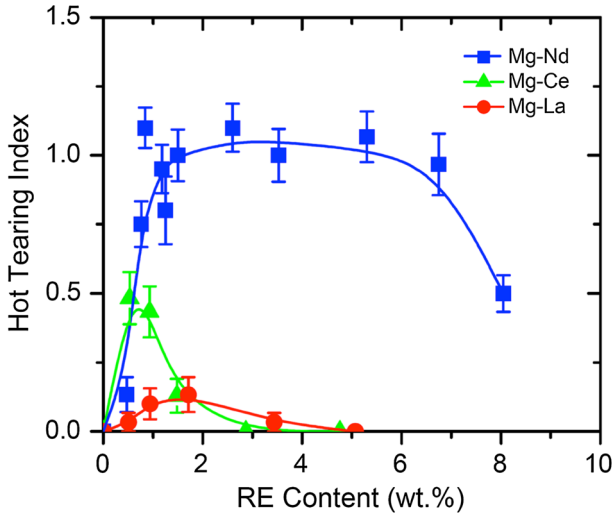


Fig. 4—HTI of the binary Mg-RE alloy series plotted against the RE content.

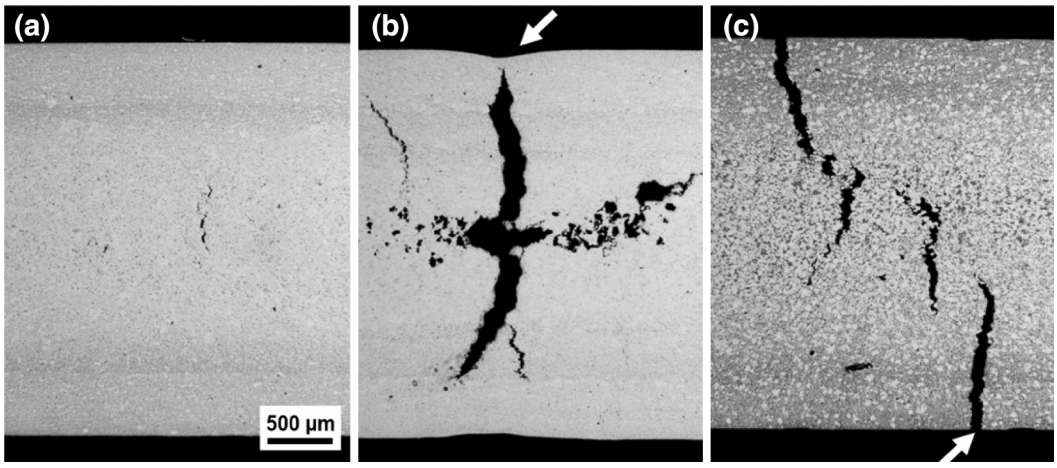


Fig. 3—Low-magnification photomicrographs of polished longitudinal cross sections through rectangular tensile test pieces that display differing degrees of hot tearing as determined by the HTI. (*a*) HTI 0, (*b*) HTI 2 (the white arrow indicates the dimple that is visible on the specimen surface), and (*c*) HTI 3 (the white arrow indicates that the crack is clearly visible in the specimen surface).

The hot-tearing susceptibility of the alloy series appears to be related to their solidification ranges with the Mg-Nd alloy system having the lowest temperature eutectic, followed by the Mg-Ce alloys, with Mg-La alloys having the highest eutectic temperatures (Table I). A further observation is that Mg-Nd alloys have the highest eutectic composition, and hence have the lowest amount of eutectic for a particular alloy composition.

The main observation from an alloy design perspective is that most Mg-Nd binary alloys would not be acceptable for HPDC. Even at approximately 0.5 wt pct Nd, significant hot tearing is observed, and it is only above 8 wt pct that the hot-tearing susceptibility begins to decrease. The Mg-Ce alloys show some minor hot tearing at concentrations ranging approximately from 0.5 to 1 wt pct, while the Mg-La alloys showed hardly any hot-tearing susceptibility at all. Mg-Ce alloys may not be acceptable in the range from 0.5 to 1.0 wt pct, while Mg-La alloys appear to be very castable.

## IV. DEVELOPMENT OF AN *A PRIORI* HOT-TEARING INDICATOR

Virtually all hot-tearing models indicate that the final stages of solidification are the most important. Early models, such as that of Clyne–Davies,[56] described the hot-tearing susceptibility as being related to the time, t, spent in the range of fraction solid, $f_s$, where stresses can be relaxed ($f_s$ = 0.4 to 0.9) compared with the range where they cannot be relaxed ($f_s$ = 0.9 to 0.99), usually in high fraction solids, *i.e.*,

$$S_{CD} = \frac{t_{0.99} - t_{0.9}}{t_{0.9} - t_{0.4}} \quad [1]$$

In effect, this means that alloys with a large solidification range toward the end of solidification will have larger hot-tearing susceptibilities, and this is well recognized as a key factor affecting hot tearing.[57,58] Hence, although this ratio is an oversimplification, the general principal is correct, which is why it is often still used even though our understanding of hot-tearing phenomena has developed considerably since it was first posited. Some modifications and improvements have been made to this model by recognizing that the coherency point (*i.e.*, where feeding becomes interdendritic) may vary and therefore, not be specifically equal to 0.9.[2] It is also problematic in situations such as high-pressure die-casting (HPDC) where, due to the very high solidification rates, the time at the various stages of solidification is impossible to measure. Hence, it is preferable to use some more readily calculated parameter to input into a model, such as the temperature–fraction solid ($T$–$f_s$) solidification path, which is the one that actually affects the relative times in the different stages of solidification and is an approach already used by many authors.[27–29,31,58,59]

A schematic description that is now commonly used to explain hot tearing is to consider liquid feeding through a mushy zone to accommodate shrinkage occurring during solidification (Figure 5).[60] This understanding of hot tearing indicates that permeability is a key factor in determining the hot-tearing susceptibility of an alloy and has in itself has been used as an indicator of hot-tearing susceptibility.[41] The Carman-

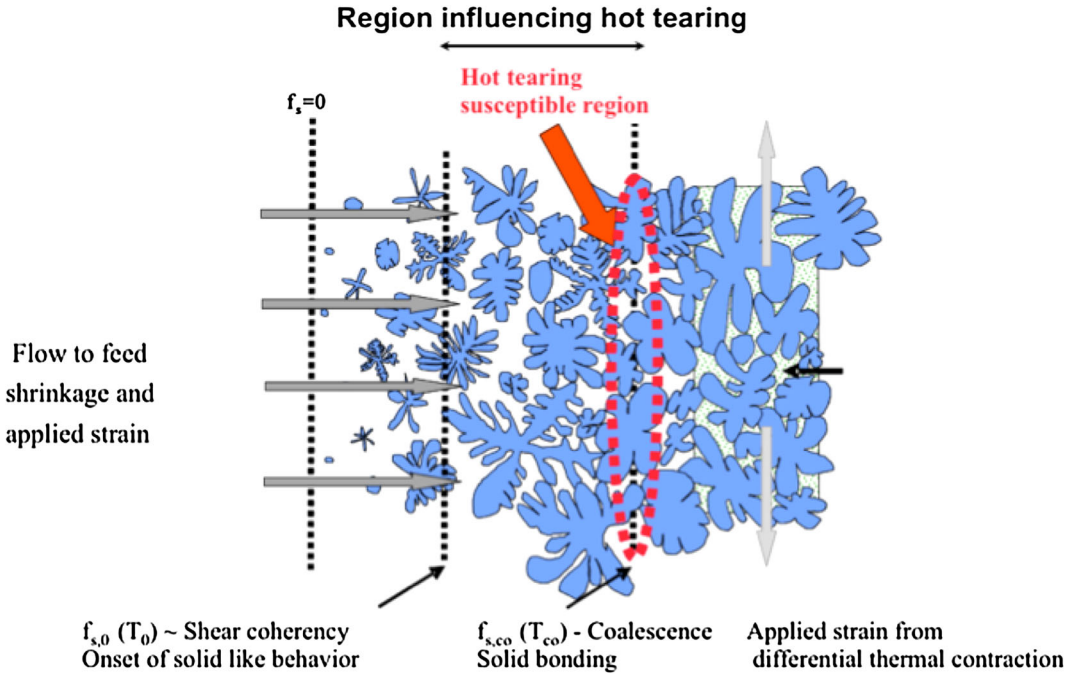


Fig. 5—Schematic showing the key factors affecting hot tearing. Adapted from Grandfield *et al.*[60]

Kozeny equation is often used,[61] where the permeability, $K$, is defined as

$$K = \frac{\lambda_2^2}{180}\frac{(1-f_s)^3}{f_s^2}, \quad [2]$$

where $\lambda_2$ is the permeability parameter, which is the secondary dendrite arm spacing when the grain morphology is dendritic, is often used to describe this mathematically.

However, there are also two key points that are particularly important during the solidification sequence. Therefore, more recently, research has been based on the assumption that the critical part of the solidification process for hot tearing is between *coherency*—the point at which feeding becomes interdendritic, *i.e.*, shrinkage must be accommodated by the flow of liquid through an established solid network—and *coalescence* when the metal has solidified sufficiently that it can act as a solid. Hence, it makes more sense to use these two points, and there have been a considerable number of studies trying to determine what they are in various systems[6,12,24–26,54,62,63] rather than considering the fraction solids used in Eq. [1], particularly for the region where the stresses can be relaxed ($f_s$ = 0.4 to 0.99).

The other important factor is the strain developed during shrinkage.[64] This is considered by another simple model for hot tearing by Zhang and Singer.[65] They considered a critical temperature range and the strain in one-dimension, which is probably reasonable for most hot-tearing situations where the tear will propagate perpendicular to a principal stress. They propose that the hot-tearing susceptibility is related to the strain

$$\varepsilon = \alpha \int dT + \beta^{1/3} \int df_s(T), \quad [3]$$

where $\alpha$ is the thermal expansion coefficient, $\beta$ is the bulk shrinkage, and the integral is taken over the critical solidification range which they define as the situation between "when the secondary dendrite arms begin to contact each other and bonds begin to form between them," which is the same as the definition given above.

In more complete models, such as the Rappaz–Drezet–Gramaud (RDG) model,[66] both the feedability of the mush and the strain caused by shrinkage are considered (although, in this case, it is the strain rate that is used as the critical parameter). Because of this, the $T$–$f_s$ curve is one of the fundamental pieces of information used, as the fraction solid evolution is known to affect the permeability of the mushy zone. The critical strain rate for hot tearing (inverse of the hot-tearing susceptibility) becomes as follows:

$$\mathrm{csr_e} = \frac{d^2}{180(1+\beta)B\mu L^2}\left[P_m + \frac{4\gamma}{\lambda_2\left(1-\sqrt[3]{f_{s,co}}\right)}\right] - \frac{V\beta A}{(1+\beta)BL}, \quad [4]$$

where

$$A = \frac{1}{T_0 - T_{co}}\int_{T_{co}}^{T_0}\frac{f_s(T)^2}{(1-f_s(T))^2}, \quad B = \frac{1}{T_0 - T_{co}}\int_{T_{co}}^{T_0}\frac{f_s(T)^2 F(T)}{(1-f_s(T))^3}, \quad F(T) - \frac{1}{T_0 - T_{co}}\int_{T_{co}}^{T} f_s(T)\cdot dt,$$

where $\lambda_2$ is the secondary dendrite arm spacing (or the equiaxed grain size depending on the grain morphology[67]), $\mu$ is the viscosity, $\gamma$ is the surface tension, $P_m$ is the metal head pressure, $\beta$ is the bulk shrinkage, $V$ is the growth rate, $L$ is the length of the mushy zone, $T_0$ is the temperature at which strain can be transferred though the mushy zone (related to $f_{s,0}$ the corresponding fraction solid), and $T_{co}$ is the solid coalescence temperature (related to $f_{s,co}$). In the case of a casting process with similar process parameters and grain size/morphology, the key alloy parameters, related to the solidification path affecting the hot tearing, are found in the integrals $A$ and $B$ and the length of the mushy zone, $L$.

One of the aims of the current article is to obtain a relatively simple indicator of hot-tearing susceptibility based on the predicted solidification path of alloys. It is clear that the RDG model predicts a lambda-curve. The solidification interval is important as it is the one that controls the length of the mushy zone, L. This means that to the first order the RDG model predicts that the hot-tearing susceptibility is proportional to the solidification interval as shown in their original article.[66] However, it is also seen that the prediction deviates substantially from that particularly showing a relatively rapid decrease in the hot-tearing behavior of the alloys as the concentration is increased above the peak. The integrals $A$ and $B$ are also very important given the bounds of the integrals (coherency and coalescence points) which are also important in the prediction of the hot-tearing susceptibility. Given the permeability model and these integrals, it is interesting to see how these integrals may affect the hot-tearing susceptibility as well. To investigate this, a relatively simple alloy-dependent indicator, based on integral $A$ in Eq. [4], but of a similar form to the permeability, $K$ (Eq. [2]) and integral $B$ in Eq. [4] of hot tearing is given below:

$$S_{ht1} = \int_{T_0}^{T_{co}}\frac{f_s(T)^2}{(1-f_s(T))^2}\cdot dT, \quad [5]$$

where $T_0$ is the temperature at which coherency occurs, and $T_{co}$ is the temperature at which coalescence has been achieved.[54,68] It should be noted that changing the index of the denominator from 2 to 3 similar to Eq. [2] provides similar relative results to the equation as given, but of a different magnitude.

An alternative simple parameter, based on improvements to the Clyne–Davies model is as follows. It is assumed that solidification occurs in a way that the heat extraction rate is constant; that it is clear that the

important points to consider are the coherency and coalescence points; and that the solidification profile between those two points are important (rather than just a linear tie-line). Hence, a useful indicator for comparing the hot-tearing resistance between alloys can be proposed:

$$S_{ht2} = \int_{T_0}^{T_{co}} f_s(T) \cdot dT \qquad [6]$$

One of the greatest advantages of this approach is that rather than the linear average inherent in the Clyne–Davies model and its improvements,[2,32] the effect of the tail end of the solidification profile, *i.e.*, at higher fractions solid, increases the hot-tearing parameter more than that for the lower fractions solid, as feeding becomes more difficult.

To use these hot-tearing indicators, two important additional pieces of information are required: (1) the temperature-fraction solid profile; and (2) a determination of the actual bounds of the integral, *i.e.*, the coherency and coalescence points.

The temperature fraction solid profiles can be either generated from CALPHAD prediction software or in the case of simple systems, such as binary alloys, can be generated using parameters from the binary phase diagrams and the Scheil–Gulliver equation:[69]

$$c_s = kc_0(1 - f_s)^{k-1}, \qquad [7]$$

where $c_s$ in the composition of the solid; $k$ is the partition coefficient, *i.e.*, the ratio between the composition of the solid and liquid; and $c_o$ is the alloy composition. It gives a reasonable estimate of the nonequilibrium solidification behavior of most alloys without the need for diffusion data.[43,70,71] Chia *et al.*[43] have already developed these relationships for the alloys of the current study and validated the model. This is especially important in HPDC as the use of thermal analysis techniques at such high cooling rates is very difficult if not impossible. Typically, the Scheil–Gulliver model provides better predictions at higher cooling rates.[72]

The integral bounds for coherency and coalescence are more difficult to determine, particularly in HPDC. There has been substantial research devoted to trying to understand and measure both of these points in conventional casting conditions. Instrumented hot tearing of constrained bars has become common place in the research community;[30,58,73,74] however, it is not possible to measure load responses or contraction during solidification in HPDC. Hence, estimates are required as to the fraction solid at which these points occur.

Shear coherency has been shown to be dependent on grain size and morphology, but in the case of hot-tearing tensile coherency is more important and will occur much later in solidification. Rappaz *et al.*[66] integrated from $f_{s,0} = 0$. When considering a columnar case feeding down the primary arms, this makes sense. However, for equiaxed grains, this is no longer valid as mass feeding, where the solid grains can move with the liquid, occurs well into solidification.[63] A value worth considering is when spherical grains touch at a fraction solid of 0.74, so that one value that is used in this article is 0.7. Another one, which is present in some of the models, is 0.9, which seems like a very high fraction solid to be a barrier to interdendritic feeding, but it could be that it is only at this fraction solid that the feeding becomes difficult. While it appears to be quite uncertain what the value of the coherency point should be, previous studies, [54,68] while determining the sensitivity of model predictions to this parameter, have shown that it has very little effect on the final result. This is because most of the feeding constriction and the strain accumulation occur in the final 10 pct of solidification.

The value of coalescence, however, is very important as it affects the results substantially. Moreover, it has also been more extensively researched, and a value of between 0.97 and 0.99 has been suggested previously.[2,56,62,66,75] There are some that suggest that hot tearing can be observed at values closer to 0.9,[59,76] which may be because hot tearing must occur before the range from 0.97 to 0.99. Even within such values, the concentration at which the peak hot-tearing susceptibility occurs changes significantly, and it appears that the alloy composition can change the value in more complex systems.[54,68]

## V. HOT-TEARING INDICATOR FOR Mg-La, Mg-Ce, AND Mg-Nd ALLOYS

Besides characterizing the hot-tearing response in Mg-RE alloys, it was decided to use the data generated in this article to consider the best and the simplest HTI for predicting the relative susceptibility of alloys to hot tearing.

The parameters, $S_{ht1}$ and $S_{ht2}$—with $f_{s,0}$ being 0 and $f_{s,co}$ being 0.98—are compared in Figure 6 for the Mg-Nd alloys. Both predict a peak at about 1 wt pct for the Mg-Nd system, but $S_{ht2}$ appears to give a slower

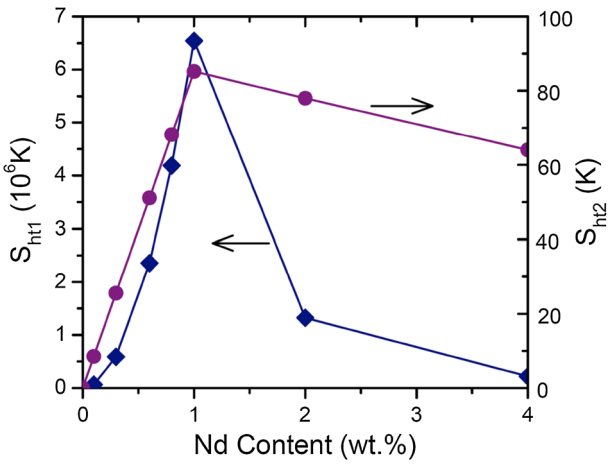


Fig. 6—A comparison of the predictions of the two hot-tearing parameters in the Mg-Nd system with $f_{s,0} = 0$ and $f_{s,co} = 0.98$.

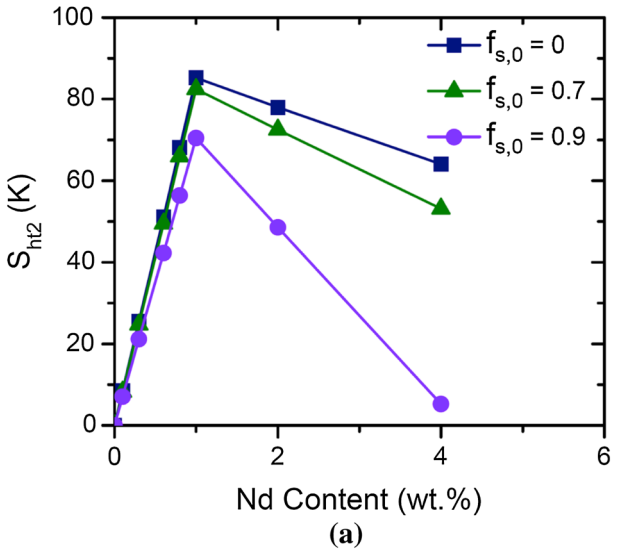


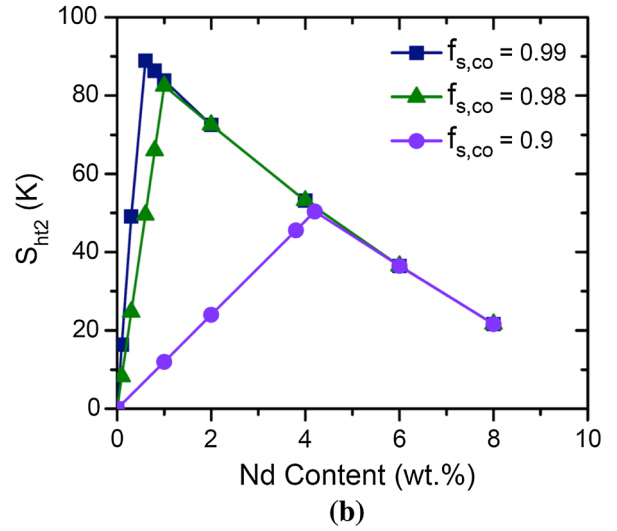


Fig. 7—Predictions of hot tearing of Mg-Nd system using (*a*) $S_{ht2}$ for three different values of $f_{s,0}$: 0, 0.7, and 0.9 with a $f_{s,co}$ = 0.98; and (*b*) $S_{ht2}$ for three different values of $f_{s,co}$: 0.9, 0.98, and 0.99 with a $f_{s,0}$ = 0.7.

reduction in the hot-tearing susceptibility with the increasing alloy content. The slower rate of decrease in hot-tearing susceptibility is more representative of the results given in Figure 4, especially for Mg-Nd. Interestingly, the literature shows some examples of the hot-tearing susceptibility decreasing slowly after the peak [4,30,39] and others more rapidly.[28,30,40]

Before settling on the values for the integral bounds, it was decided to do a sensitivity analysis to see how the changes in $f_{s,0}$ and $f_{s,co}$ affect the results. Increasing the $f_{s,0}$ value from 0 to 0.9 (Figure 7(a)) has no effect on the composition at which the peak occurs and has little influence on the peak maximum, but it does have a significant effect on how rapidly the hot-tearing susceptibility is predicted to decrease as the alloy content increases. Interestingly, this very effect was observed by Dodd *et al.*[40] between an unfed casting and one fed by a riser. A value of 0.7 will be used here as it showed a

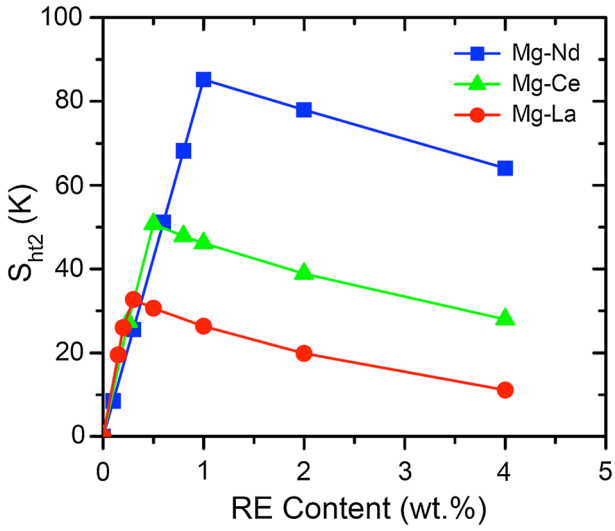


Fig. 8—Predictions of $S_{ht2}$ for $f_{s,0}$ = 0.7, $f_{s,co}$ = 0.98 for the three Mg-RE alloy systems.

relatively moderate decrease in hot-tearing susceptibility after the peak similar to the results, and it is close to the impingement value of spheres, which represents a good estimate for the only slightly dendritic grain morphology observed in the HPDC microstructure.[43]

Changing $f_{s,co}$ has a different but more significant effect (Figure 7(b)). The concentration at the peak of the hot tearing changes considerably, with an $f_{s,co}$ of 0.99 predicting a peak at approximately 0.6 pct Nd, of 0.98 about 1.0 pct Nd, and for an $f_{s,co}$ of 0.9, the peak is lower and predicted at about 4.2 pct Nd. Hence, small changes can have a substantial affect on the predictions of the peak hot-tearing resistance. Consequently, a value of 0.98 will be used, as this is in the middle of the 0.97 to 0.99 range that previous authors[2,56,62,67,76] have identified, and it fits closely with the peak in the hot tearing observed in Figure 4.

The predictions of the hot-tearing susceptibility parameter, $S_{ht2}$, with $f_{s,0}$ = 0.7 and $f_{s,co}$ = 0.98, for the Mg-La, Mg-Ce, and Mg-Nd alloy systems are shown in Figure 8. It can be seen that the Mg-Nd alloys have the highest peak at approximately 1.0 wt pct Nd with a relatively moderate decrease in hot-tearing propensity as the alloy content increases. The Mg-Ce alloys display a slightly earlier, lower peak than the Mg-Nd alloys with the hot-tearing susceptibility decreasing at higher concentrations. The earlier, lower, peak seems to fit better with the experimental data, although virtually no hot tearing is observed at concentrations greater than 2.5 pct (Figure 4). The predicted peak for the Mg-La alloys was lower still. This agrees with the experimental data in that very little hot tearing was observed for these alloys, even if the peak is of a different relative height and composition between the predicted and experimental results.

Figure 9(a) compares the temperature–fraction solid curves as predicted from the Scheil–Gulliver equation for each of Mg-Nd, Mg-Ce, and Mg-Nd systems at 1 wt pct concentration. It can be seen that the temperature range over which the solidification between the fractions solid of 0.7 and 0.98 is much greater in the Mg-Nd alloy

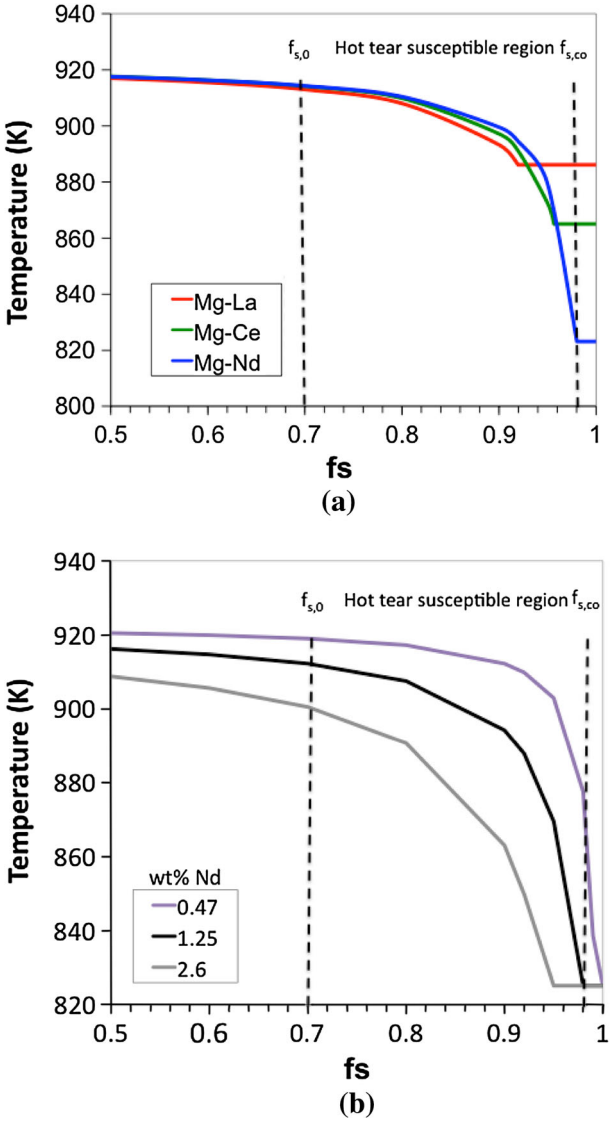


Fig. 9—Predicted temperature–fraction solid curves for (*a*) Mg-1 wt pct La, Mg-1 wt pct Ce, and Mg-1 wt pct Nd; and (*b*) Mg-0.47 wt pct Nd, Mg-1.26 wt pct Nd, and Mg-2.6 wt pct Nd alloys.

than in the Mg-Ce, while the Mg-La alloy has the shortest freezing range. In Figure 9(b), the temperature–fraction solid profiles for alloys from below, at, and above the peaks in hot-tearing susceptibility are compared for the Mg-Nd alloy system. Again, it is seen that the alloy with the highest hot-tearing susceptibility (1.25Nd) has a longer freezing range between $f_s = 0.7$ and 0.98 than the 0.47Nd alloy which does not contain a significant eutectic volume, whereas the 2.6Nd alloy which forms considerable eutectic.

These results show the importance of the solidification range of alloys near the end of solidification when considering the hot-tearing susceptibility of alloy systems. It should be pointed out that these alloys have very similar eutectics and eutectic phases[43] with the Mg-La and Mg-Ce alloys both having a α-Mg-$REMg_{12}$ eutectic, while the Mg-Nd alloy has the metastable α-Mg-$REMg_3$ eutectic.[77] However, it is noted that the Mg-Al alloy system, which the authors have cast a number of times into the same die under similar casting conditions, has never shown evidence of significant hot tearing even though its eutectic temperature is lower than all three Mg-RE systems at 705 K (432 °C).[78] On the other hand, Zn-rich Mg alloys, with an even lower eutectic temperature, ~613 K (340 °C) have been the most susceptible to hot tearing, which the authors have tested.[51,79] Similarly, as reported by Rossenberg *et al.*,[39] binary Al systems did not always show peaks in hot tearing related to the solidification range. Hence, it appears that there are other factors such as the type and probably the morphology of the eutectic that may also affect the hot-tearing response.[54]

It is clear that Nd-rich Mg alloys, which are suitable for sand casting and permanent mold casting,[36,37] are not suitable for HPDC because of their susceptibility to hot tearing. However, it appears that Mg-La alloys may provide a suitable base for developing HPDC alloys also giving some favorable aspects of castability such as a more coherent skin,[80,81] although they have the lowest creep resistance among the three alloy systems.[44]

## VI. CONCLUSIONS

1. HPDC Mg-RE alloys show increasing hot-tearing susceptibility ranging from 1 to 2 wt pct solute additions, and then, a decrease after that point. Mg-Nd alloys have a relatively high hot-tearing susceptibility peaking at around 1 wt pct and not decreasing significantly until above 7 wt pct. Mg-Ce alloys showed some hot tearing, but very little was observed in Mg-La alloys. For these alloys, the hot-tearing susceptibility was closely related to the solidification range of the alloys, with Mg-Nd alloys having the greatest freezing range (the lowest eutectic temperature) and Mg-La alloys having the shortest freezing range (the highest eutectic temperature).
2. An *a priori* hot-tearing indicator has been used to provide a reasonable indication of the relative hot-tearing response of the alloys. The indicator involves taking the integral over the fraction solid curve, as a function of temperature, between the temperatures related to the fraction solid at which feeding becomes restricted (coherency) and that at which a three-dimensional solid-bonded material is formed (coalescence). This parameter has some advantages over those previously proposed due to a combination of its simplicity, such as its incorporation of tailored coherency and coalescence points, and ability to make accurate predictions of relative hot-tearing susceptibilities of alloys from the temperature–fraction solid curves.
3. The value of fraction solid chosen for the coherency and coalescence points is important for the prediction of the hot-tearing response. The hot-tearing susceptibility is not as dependant on the coherency point where it only has a minor effect on the peak of the lambda-curve but does affect the slope of the decrease after the peak. The coalescence point substantially changes the position and height of the peak.

## ACKNOWLEDGMENTS

The CAST Co-operative Research Centre was established under, and was supported in part by the Australian Governments Co-operative Research Centre program. The authors would like to thank Maya Gershenson and Andrew Yob of CSIRO for operating the high-pressure die-casting machine to produce the samples evaluated in this publication. ME also thanks Dr. Dacian Tomus of Monash University for fruitful discussions on this model.

## REFERENCES

1. L. Bichler and C. Ravindran: *Mater. Des.*, 2010, vol. 31, pp. S17–S23.
2. L. Katgerman: *JOM*, 1982, vol. 34, pp. 449–55.
3. T.W. Clyne: *Solidification Cracking of Aluminium Alloys*, The University of Cambridge, Cambridge, 1976.
4. J. Campbell and T.W. Clyne: *Cast Met.*, 1991, vol. 3 (4), pp. 224–26.
5. M.O. Pekguleryuz, S. Lin, E. Ozbakir, D. Temur, and C. Aliravci: *Int. J. Cast Met. Res.*, 2010, vol. 23 (5), pp. 310–20.
6. M. Rappaz, A. Jacot, and W.J. Boettinger: *Metall. Mater. Trans. A*, 2003, vol. 34A, pp. 467–79.
7. N. Wang, S. Mokadem, M. Rappaz, and W. Kurz: *Acta Mater.*, 2004, vol. 52 (11), pp. 3173–82.
8. D.J. Lahaie and M. Bouchard: *Metall. Mater. Trans. B*, 2001, vol. 32B, pp. 697–705.
9. M. M'Hamdi, R. Krieft, D. Mortensen, A. Mo, and J. Rabenburg: *Aluminium*, 2002, vol. 78 (10), p. 847.
10. D. Fabrègue, A. Deschamps, M. Suéry, and J.-M. Drezet: *Acta Mater.*, 2006, vol. 54, pp. 5209–20.
11. M.G. Pokorny, C.A. Monroe, C. Beckermann, Z. Zhen, and N. Hort: *Metall. Mater. Trans. A*, 2010, vol. 41A, pp. 3196–3207.
12. D.G. Eskin, Suyitno, J.F. Mooney, and L. Katgerman: *Metall. Mater. Trans. A*, 2004, vol. 35A, pp. 1325–35.
13. S. Lin, C. Aliravci, and M.O. Pekguleryuz: *Metall. Mater. Trans. A*, 2007, vol. 38A, pp. 1056–68.
14. Ø. Nielsen, L. Arnberg, A. Mo, and H. Thevik: *Metall. Mater. Trans. A*, 1999, vol. 30A, pp. 2455–62.
15. S. Li, K. Sadayappan, and D. Apelian: *Metall. Mater. Trans. A*, 2013, vol. 44A, pp. 614–23.
16. Suyitno, D.G. Eskin, V.I. Savran, and L. Katgerman: *Metall. Mater. Trans. A*, 2004. vol. 35, pp. 3551–61.
17. M. M'Hamdi, A. Mo, and H.G. Fjaer: *Metall. Mater. Trans. A*, 2006, vol. 37A, pp. 3069–83.
18. A. Stangeland, A. Mo, M. M'Hamdi, D. Viano, and C.J. Davidson: *Metall. Mater. Trans. A*, 2006, vol. 37A, pp. 705–14.
19. A. Stangeland, A. Mo, and D.G. Eskin: *Metall. Mater. Trans. A*, 2006, vol. 37A, pp. 2219–29.
20. Suyitno, W.H. Kool, and L. Katgerman: *Metall. Mater. Trans. A*, 2009, vol. 40A, pp. 2388–2400.
21. H. Hao, D.M. Maijer, M.A. Wells, A. Phillion, and S.L. Cockcroft: *Metall. Mater. Trans. A*, 2010, vol. 41A, pp. 2067–77.
22. M. M'Hamdi and A. Mo: *Mater. Sci. Eng. A*, 2005, vols. 413–414, pp. 105–08.
23. A.B. Phillion, S.L. Cockroft, and P.D. Lee: *Mater. Sci. Eng. A*, 2008, vol. 491 (1–2), pp. 237–47.
24. A. Stangeland, A. Mo, Ø. Nielsen, D.G. Eskin, and M. M'Hamdi: *Metall. Mater. Trans. A*, 2004, vol. 35A, pp. 2903–15.
25. S. Vernéde and M. Rappaz: *Philos. Mag.*, 2006, vol. 86 (24), pp. 3779–94.
26. S. Vernéde, P. Jarry, and M. Rappaz: *Acta Mater.*, 2006, vol. 54, pp. 4023–34.
27. P. Gunde, A. Schiffl, and P.J. Uggowitzer: *Mater. Sci. Eng. A*, 2010, vol. 527, pp. 7074–79.
28. Z.G. Wang, Y. Huang, A. Srinivasan, Z.K. Liu, F. Beckmann, K.U. Kainer, and N. Hort: *Mater. Des.*, 2013, vol. 47, pp. 90–100.
29. L. Zhou, Y.-D. Huang, P.-L. Mao, K.U. Kainer, Z. Liu, and N. Hort: *Int. J. Cast Met. Res.*, 2011. vol. 24 (3/4), pp. 170–76.
30. G. Cao and S. Kau: *Mater. Sci. Eng. A*, 2006, vol. 417, pp. 230–38.
31. X. Yan and J.C. Lin: *Metall. Mater. Trans. B*, 2006, vol. 37B, pp. 913–18.
32. N. Hatami, R. Babaei, M. Dadashzadeh, and P. Davami: *J. Mater. Process. Technol.*, 2008, vol. 205 (2), pp. 506–13.
33. Suyitno, W.H. Kool, and L. Katgerman: *Metall. Mater. Trans. A*, 2005. vol. 36A, pp. 1537–46.
34. I. Farup and A. Mo: *Metall. Mater. Trans. A*, 2000, vol. 31A, pp. 1461–72.
35. A. Luo: *Int. Mater. Rev.*, 2004, vol. 49 (1), pp. 13–30.
36. F. Penghuai, P. Liming, J. Haiyan, C. Jianwei, and Z. Chunquan: *Mater. Sci. Eng. A*, 2008, vol. 486, pp. 183–92.
37. C.J. Bettles, M.A. Gibson, and S.M. Zhu: *Mater. Sci. Eng. A*, 2009, vol. 505 (1–2), pp. 6–12.
38. A.C. Hänzi, A.S. Sologubenko, and P.J. Uggowitzer: *Int. J. Mater. Res.*, 2009, vol. 100 (8), pp. 1127–36.
39. R.A. Rossenberg, M.C. Flemings, and H.F. Taylor: *AFS Trans.*, 1960, vol. 68, pp. 518–28.
40. R.A. Dodd, W.A. Pollard, and J.W. Meier: *AFS Trans.*, 1957, vol. 65, pp. 110–17.
41. J.A. Spittle and S.G. Brown: *Mater. Sci. Technol.*, 2005, vol. 21 (9), pp. 1–7.
42. A. Srinivasan, Z. Wang, Y. Huan, F. Beckmann, K.U. Kainer, and N. Hort: *Metall. Mater. Trans. A*, 2013, vol. 44A, pp. 2285–98.
43. T.L. Chia, M.A. Easton, S.M. Zhu, M.A. Gibson, N. Birbilis, and J.F. Nie: *Intermetallics*, 2009, vol. 17, pp. 481–90.
44. S.M. Zhu, M.A. Gibson, M.A. Easton, and J.F. Nie: *Scripta Mater.*, 2010, vol. 63 (7), pp. 698–703.
45. N. Birbilis, M.K. Cavanaugh, A.D. Sudholz, S. Zhu, M.A. Easton, and M.A. Gibson: *Corros. Sci.*, 2011, vol. 53 (1), pp. 168–76.
46. N. Birbilis, M.A. Easton, A.D. Sudholz, S.M. Zhu, and M.A. Gibson: *Corros. Sci.*, 2009, vol. 51 (3), pp. 683–89.
47. L.L. Rokhlin: *Magnesium Alloys Containing Rare Earth Metals*, Taylor & Francis, New York, 2003, pp. 159–64.
48. M.A. Easton, K. Strobel, S. Zhu, M.A. Gibson, and J.F. Nie: *Mater. Sci. Forum*, 2010, vols. 654–656, pp. 683–86.
49. D. Warrington and D.G. McCartney: *Cast Met.*, 1989, vol. 2, pp. 134–43.
50. J. Spittle and A. Cushway: *Met. Technol.*, 1983, vol. 10, pp. 6–13.
51. M. Easton, T. Abbott, J.F. Nie, and G. Savage: *Magnesium Technology*, TMS, Warrendale, 2008, pp. 323–28.
52. W. Xiao, M.A. Easton, S. Zhu, M.S. Dargusch, M.A. Gibson, S. Jia, and J.F. Nie: *Adv. Eng. Mater.*, 2012, vol. 14 (1–2), pp. 68–76.
53. S. Gavras, M.A. Easton, M.A. Gibson, S. Zhu, and J.F. Nie: *J. Alloy. Compd.*, 2014, vol. 597, pp. 21–29.
54. L. Sweet, M.A. Easton, J.A. Taylor, J. Grandfield, C.J. Davidson, L. Lu, M.J. Couper, and D.H. StJohn: *Metall. Mater. Trans. A*, 2013, vol. 44A, pp. 5396–407.
55. J. Campbell: *Castings*, 2nd ed., Butterworth-Heinemann, Oxford, 2003, p. 328.
56. T.W. Clyne and G.J. Davies: *British Foundryman*, 1981, vol. 74, pp. 65–73.
57. L. Bichler, C. Ravindran, and D. Sediako: *Can. Metall. Q.*, 2009, vol. 48 (1), pp. 81–90.
58. G. Cao and S. Kou: *Metall. Mater. Trans. A*, 2006, vol. 37A, pp. 3647–63.
59. G. Cao, I. Haywood, and S. Hou: *Metall. Mater. Trans. A*, 2010, vol. 41A, pp. 2139–50.
60. J.F. Grandfield, C.J. Davidson, and J.A. Taylor: *Light Metals 2001*, Minerals and Materials Society, The Metals, 2001, pp. 911–917.
61. S.G. Brown, J.A. Spittle, D.J. Jarvis, and R. Walden-Bevan: *Acta Mater.*, 2002, vol. 50 (6), pp. 1559–69.
62. Y.F. Guven and J.D. Hunt: *Cast Met.*, 1988, vol. 1, pp. 104–11.
63. A.K. Dahle, S. Instone, and T. Sumitomo: *Metall. Mater. Trans. A*, 2003, vol. 34A, pp. 105–13.
64. C. Puncreobutr, P.D. Lee, R.W. Hamilton, B. Cai T. Connolley: *Metall. Mater. Trans. A*, 2013, vol. 44A, pp. 5389–95.
65. J. Zhang and R.F. Singer: *Acta Mater.*, 2002, vol. 50, pp. 1869–79.
66. M. Rappaz, J.-M. Drezet, and M. Gremaud: *Metall. Mater. Trans. A*, 1999, vol. 30A, pp. 449–55.
67. M.A. Easton, H. Wang, J.F. Grandfield, D.H. StJohn, and E. Sweet: *Mater. Forum*, 2004, vol. 28, pp. 224–29.
68. M.A. Easton, H. Wang, J. Grandfield, C.J. Davidson, D.H. StJohn, L. Sweet, and M.J. Couper: *Metall. Mater. Trans. A*, 2012, vol. 43A, pp. 3227–38.

69. M.E. Glicksman and R.N. Hills: *Philos. Mag. A*, 2001, vol. 81 (1), pp. 153–59.
70. D. Mirković and R. Schmid-Fetzer: *Metall. Mater. Trans. A*, 2009, vol. 40A, pp. 958–73.
71. J.R. TerBush, R.R. Adarapurapu, J.W. Jones, and T.M. Pollock: in *Magnesium Technology 2009*, E.A. Nyberg, *et al.*, eds., The Metals, Minerals and Materials Society, Warrendale, PA/San Fransisco, 2009, pp. 161–65.
72. X. Doré, H. Combeau, and M. Rappaz: *Acta Mater.*, 2000, vol. 48, pp. 3951–62.
73. S. Li, K. Sadayappan, and D. Apelian: *Int. J. Cast Met. Res.*, 2011, vol. 24 (2), pp. 88–95.
74. S. Instone, D.H. StJohn, and J. Grandfield: *Int. J. Cast Met. Res.*, 2000, vol. 12, pp. 441–56.
75. S. Vernéde, J.A. Dantzig, and M. Rappaz: *Acta Mater.*, 2009, vol. 57, pp. 1554–59.
76. D.G. Eskin, Suyitno, and L. Katgerman: *Prog. Mater. Sci.*, 2004, vol. 49, pp. 629–711.
77. M.A. Easton, M.A. Gibson, D. Qiu, S.M. Zhu, J. Gröbner, R. Schmid-Fetzer, J.F. Nie, and M.X. Zhang: *Acta Mater.*, 2012, vol. 60, pp. 4420–30.
78. I.J. Polmear: *Mater. Sci. Technol.*, 1994, vol. 10 (1), pp. 1–16.
79. W. Xiao, S.M. Zhu, M.A. Easton, M. Dargusch, M.A. Gibson, and J.F. Nie: *Mater. Charact.*, 2012, vol. 65, pp. 28–36.
80. K.V. Yang, M.A. Easton, and C.H. Cáceres: *Adv. Eng. Mater.*, 2013, vol. 15 (4), pp. 302–07.
81. K.V. Yang, C.H. Caceres, M.A. Easton, and M.A. Gibson: *Kovove Materialy*, 2011, vol. 49 (3), pp. 207–12.